Spatial-to-spectral mapping in spontaneous parametric down-conversion

Silvia Carrasco, Juan P. Torres, and Lluis Torner
ICFO-Institut de Ciencies Fotoniques, and Department of Signal Theory and Communications, Universitat Politecnica de Catalunya, 08034 Barcelona, Spain

Alexander Sergienko, Bahaa E. A. Saleh, and Malvin C. Teich
Quantum Imaging Laboratory, Department of Electrical & Computer Engineering and Department of Physics, Boston University, 8 Saint Mary's Street, Boston, Massachusetts 02215, USA
(Received 13 May 2004; published 21 October 2004)

We put forward an approach for manipulating the spectral profile of entangled photon pairs. Such spectral properties are mediated by the geometry of noncollinear spontaneous parametric down-conversion and by selecting the appropriate spatial profile of the pump laser radiation. We show that one can translate spatial features imprinted in the pump beam into desired spectral profiles of the generated entangled-photon state. Particular configurations suitable for generating entangled pairs with ultranarrow spectral width and with multiple-peaked spectra are demonstrated.

DOI: 10.1103/PhysRevA.70.043817 PACS number(s): 42.50.Ar, 42.50.Dv, 42.65.Ky

Spontaneous parametric down-conversion (SPDC) is a reliable and convenient source for generating entangled-photon states and thus is currently employed in many quantum-optics applications [1]. An appropriate tailoring of the spectral properties of the entangled two-photon states is often required for efficient information encoding. For example, chromatic dispersion can cause problems for quantum cryptography schemes implemented in optical fibers, when utilizing photon pairs created via SPDC. Therefore, several schemes suitable for transmission over long distances, such as time-bin entanglement, can strongly benefit from frequency engineered—e.g., narrowband—entangled states [2]. Several other quantum-optical applications that make use of the frequency entanglement of the two photons can also benefit from such manipulation. In particular, frequency-correlated two-photon states can be used for improving the accuracy of clock synchronization [3]. Elimination of the strong correlations between the frequencies of the two photons is required for performing linear-optical logic operations [4], suppression of spectral information is crucial for experiments that make use of a portion of the state of two particles [5], and entangled photons with increased spectral width are needed for enhancing the resolution in quantum optical coherence tomography schemes [6].

Therefore, the elucidation of new physical phenomena that allow control of the spectral properties of generated entangled photon pairs is of paramount importance. To date most experimental configurations for the generation of entangled photons via SPDC in bulk materials use nearly collinear phase matching geometries, where the pump, signal, and idler photons propagate almost along the same direction. The majority of practical applications of periodically poled nonlinear materials are also limited to a collinear configuration. In this paper, we show that sufficiently noncollinear geometries, in combination with pump spatial-profile manipulation, offer new features and key opportunities for the control of entanglement.

An indication that the geometry of noncollinear SPDC affects the spectrum of the generated entangled-photon pairs is provided, e.g., in the case of counterpropagating entangled photons that are emitted in a thin waveguide [7] or a waveguide with periodic nonlinearity [8], where the frequencies of the two photons were found to be manipulable from frequency anticorrelated to frequency correlated by modifying the temporal and spatial characteristics of the pump beam [9]. In addition, using the transverse momentum of the photons in noncollinear geometries allows the engineering of spectrally uncorrelated pairs of photons, as recently suggested [10].

Here we show that using a specific noncollinear configuration of the parametric interaction, together with specially designed spatial profiles of the pump beam, allows tailoring of the spectral properties of the two-photon state over a wide range of possibilities. The selection of the dispersive properties of the material, including electing a particular type of phase matching, can further enlarge the parameter space available for engineering entangled-photon states [4]. To illustrate the potential of the method put forward here, we show that entangled-photon states with spectra of arbitrary shapes and substantially reduced width can be constructed by manipulating the pump beam profile within a noncollinear geometry.

We consider a nonlinear optical crystal of length L with periodically modulated orientation of the second-order nonlinearity, illuminated by a laser pump beam propagating in the z direction (Fig. 1). The two-photon quantum state $|\Psi\rangle$ at the output of the nonlinear crystal, within first-order perturbation theory, is given by

$$|\Psi\rangle = |0,0\rangle - (i/\hbar) \int_0^\tau dt H_I(t)|0,0\rangle, \tag{1}$$

where $|0,0\rangle$ is the vacuum state, τ is the interaction time, and $H_I(t)$ is the effective Hamiltonian in the interaction picture, given by [11]

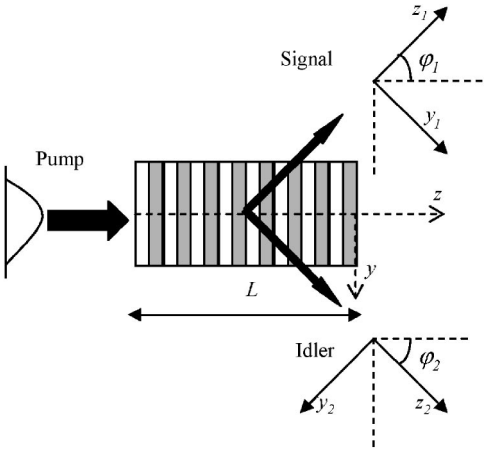

FIG. 1. Schematic of a noncollinear spontaneous parametric down-conversion process in a QPM nonlinear grating.

$$H_I = \epsilon_0 \int_V dV \chi^{(2)} \hat{E}_p^+ \hat{E}_s^- \hat{E}_i^- + \text{c.c.}, \tag{2}$$

where ϵ_0 is the permittivity of free space, $\chi^{(2)}$ is the second-order nonlinear susceptibility tensor, V is the volume of the crystal illuminated by the pump beam, $\hat{E}_p^+$ refers to the positive-frequency part of the pump electric-field operator, and $\hat{E}_{s,i}^-$ refer to the negative-frequency parts of the signal and idler electric-field operators, respectively. The profile of the paraxial pump beam, which is treated classically, is expanded in plane waves as

$$E_p(\mathbf{x},z,t) = \int d\mathbf{q}_p \overline{E}_p(\mathbf{q}_p) \exp[ik_p z + i\mathbf{q}_p \cdot \mathbf{x} - i\omega_p^0 t] + \text{c.c.}, \tag{3}$$

where $\mathbf{x}=(x,y)$ is the position in the transverse plane, z is the propagation direction of the pump beam, $\mathbf{q}_p$ is the transverse momentum, ω_p^0 is the angular frequency of the pump beam, $k_p(\mathbf{q}_p)=\sqrt{(\omega_p^0 n_p/c)^2-|\mathbf{q}_p|^2}$ is the longitudinal wave number inside the crystal, n_p is the refractive index at the pump wavelength, and $\overline{E}_p(\mathbf{q}_p)$ represents the spatial amplitude distribution of the pump beam in momentum space. We restrict ourselves to the case of a cw pump and to configurations with negligible Poynting vector walk-off, as is the case for quasi-phase-matched crystals. The results can be extended to more general settings.

To elucidate the spatial structure of the two-photon state in the noncollinear geometry, we define $x_{1,2}=x$, $y_{1,2}=y\cos\varphi_{1,2}+z\sin\varphi_{1,2}$, and $z_{1,2}=z\cos\varphi_{1,2}-y\sin\varphi_{1,2}$, where $\varphi_{1,2}$ are the angles formed by the direction of propagation of the pump beam, z, and the direction of propagation of the signal, z_1, and idler photons, z_2, respectively (see Fig. 1). Thus, the electric-field amplitude operator corresponding to the signal photon can then be written as

$$\hat{E}_s^-(\mathbf{x}_1,z,t) \propto \int d\omega_s d\mathbf{p} \exp\{-i\mathbf{p}\cdot\mathbf{x}_1 - ik_s z_1 + i\omega_s t\} \hat{a}_s^\dagger(\omega_s,\mathbf{p}), \tag{4}$$

where $\mathbf{x}_1=(x_1,y_1)$, $\mathbf{p}=(p_x,p_y)$ is the transverse momentum for the signal photon, $k_s(\mathbf{p})=[(\omega_s n_s/c)^2-|\mathbf{p}|^2]^{1/2}$ is the longitudinal wave number, $\hat{a}_s^\dagger$ is the creation operator for a photon with momentum $\mathbf{p}$ and frequency ω_s, and n_s is the refractive index inside the nonlinear crystal at the signal wavelength. The electric-field operator of the idler photon is similarly written, substituting $\mathbf{p}$ by the transverse momentum $\mathbf{q}=(q_x,q_y)$. The quantum state of the two-photon is given by [12]

$$|\Psi\rangle = \int d\omega_s\, d\omega_i d\mathbf{p} d\mathbf{q} \Phi(\omega_s,\omega_i,\mathbf{p},\mathbf{q}) \hat{a}_s^\dagger(\omega_s,\mathbf{p}) \hat{a}_i^\dagger(\omega_i,\mathbf{q}) |0,0\rangle, \tag{5}$$

where the state function is

$$\Phi(\omega_s,\omega_i,\mathbf{p},\mathbf{q}) = \overline{E}_p(p_x+q_x,\Delta_0)\text{sinc}(\Delta_k L/2)\exp(-i\Delta_k L/2). \tag{6}$$

In this expression, $\Delta_0=p_y\cos\varphi_1+q_y\cos\varphi_2-k_s\sin\varphi_1-k_i\sin\varphi_2$ comes from the phase-matching condition along the transverse y direction, $\Delta_k=k_p-k_s\cos\varphi_1-k_i\cos\varphi_2-p_y\sin\varphi_1-q_y\sin\varphi_2-2\pi/\Lambda$ comes from the phase matching condition along the longitudinal z direction, and

$$k_p = [(\omega_p^0 n_p/c)^2 - (p_x+q_x)^2 - (\Delta_0)^2]^{1/2}. \tag{7}$$

Here, Λ is the period of the modulation of the nonlinearity of the crystal in the z direction when quasi-phase-matching (QPM) is used. For convenience, the signal and idler frequencies are written as $\omega_s=\omega_s^0+\Omega_s$ and $\omega_i=\omega_i^0+\Omega_i$, respectively, where $\omega_{s,i}^0$ are the central frequencies, and $\Omega_{s,i}$ are the angular frequency deviations about the central frequencies. The central frequencies satisfy $\omega_p^0=\omega_s^0+\omega_i^0$, together with, for a cw pump beam, $\Omega_i=-\Omega_s$.

The sought after spectral properties of the state function can be extracted by measuring the function

$$\Psi(\Omega_s) = \Phi(\Omega_s,-\Omega_s,\mathbf{p}=0,\mathbf{q}=0), \tag{8}$$

which can be observed experimentally with the signal and idler photons traversing an appropriate $2f$ optical system [12]. Note that more general detection schemes that make use of different modal decompositions of the down-converted photons—i.e., projection into Gaussian modes with monomode optical fibers—are also possible. In such cases, Eq. (6) has to be integrated into the required modes. Expression (8) contains the central physical result presented here. To make it apparent, we make use of the approximation [13] $k_s=k_s^0+N_s\Omega_s+(1/2)D_s\Omega_s^2$ and $k_i=k_i^0+N_i\Omega_i+(1/2)D_i\Omega_i^2$ to obtain

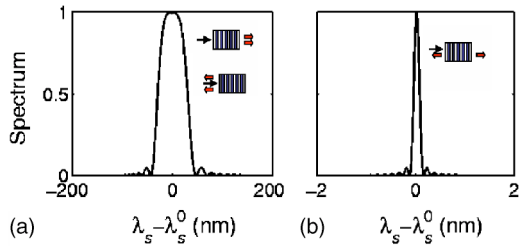

FIG. 2. Spectrum $|\Psi|^2$ for different degenerate SPDC processes. The insets sketch the different nonlinear interaction geometries. (a) Collinear forward, $\varphi_1=\varphi_2=0°$ or backward, $\varphi_1=\varphi_2=180°$. (b) Collinear counterpropagating, $\varphi_1=0°$, $\varphi_2=180°$. The twin photon source is a PPLN sample of length $L=1$ mm and the wavelength is $\lambda_p^0=406$ nm.

$$\Psi(\Omega_s) \approx \overline{E}_p(0,\alpha\Omega_s)\mathrm{sinc}\left\{\frac{(\beta\Omega_s+\gamma\Omega_s^2)L}{2}\right\} \times\exp\left\{-i\frac{(\beta\Omega_s+\gamma\Omega_s^2)L}{2}\right\}, \tag{9}$$

where $\alpha=N_s\sin\varphi_1-N_i\sin\varphi_2$, $\beta=N_i\cos\varphi_2-N_s\cos\varphi_1$, and $\gamma=(1/2)D_s\cos\varphi_1+(1/2)D_i\cos\varphi_2$ are material parameters that depend on the nonlinear crystal. The important result put forward by Eq. (9) is that the spectral properties of the down-converted photons depend on the shape of the pump beam, on the length and dispersion properties of the nonlinear crystal, and on the specific directions of propagation of the signal and idler beams, thus opening the door to obtaining desired spectral features by using the geometry of the noncollinear interaction. Equation (9) contains three terms. The first term depends on the amplitude distribution of the pump beam, scaled by the factor α, and it is independent of the crystal length. The second and third terms depend only on the crystal itself, its length, material characteristics, and type of phase matching.

We present a few examples that illustrate the potential of the technique. Figures 2 and 3 show the spectral profile for several configurations in interactions for degenerate frequency down-conversion ($\omega_p^0=2\omega_s^0=2\omega_i^0$). The period Λ of the QPM grating is then given by

$$\Lambda=\frac{m\lambda_p^0}{n_p-(n_s/2)\cos\varphi_1-(n_i/2)\cos\varphi_2}, \tag{10}$$

where $\lambda_p^0=2\pi c/\omega_p^0$ is the wavelength of the pump beam and m is the order of the QPM grating. The QPM structure is only used to obtain phase matching between the interacting waves. Other types of phase matching can also be used, such as type-I birefringent phase matching in BBO or $LiIO_3$, where one can obtain large angles of emission, φ_1 and φ_2, with no spatial walk-off. In actual materials, expression (10) yields very small domain periods for first-order QPM. For example, in PPLN or PPKTP, for $\varphi_1=-\varphi_2=90°$, one needs periods well below 1 μm. However, phase matching can be achieved by employing higher-order QPM interactions, thus with larger periods. This comes at the expense of decreasing the efficiency of the down-conversion process—i.e., $d_{eff}(m)=d_{eff}(m=1)/m$—but still with nonlinear coefficients similar to those obtained with nonlinear crystals currently used—e.g., critically phase-matched β-barium borate. The periods required to fulfill these conditions are well within the current technological state of the art [14].

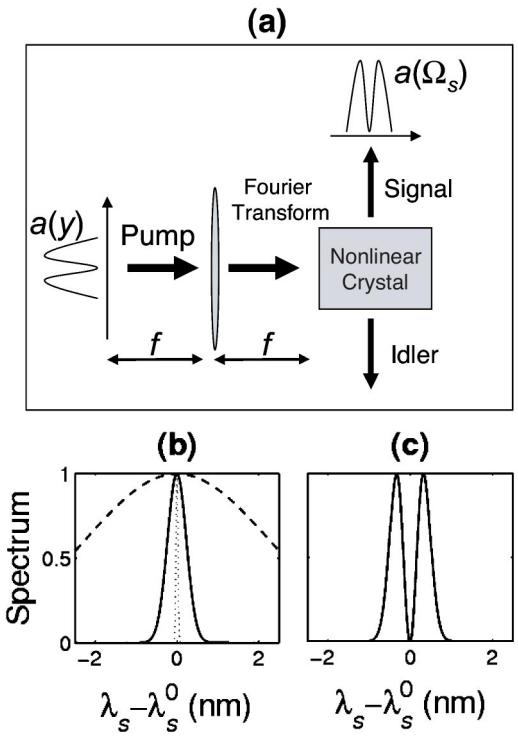

FIG. 3. Spectrum $|\Psi|^2$ for different degenerate SPDC processes in a transverse-emitting configuration, $\varphi_1=-\varphi_2=90°$. (a) General configuration for mapping the spatial shape of the pump beam into frequency distributions of the down-converted photons. In (b) the pump beam is Gaussian with $w_0=10$ μm (dashed lines), $w_0=100$ μm (thick solid line), and $w_0=1$ mm (dotted line). In (c) the pump beam is a HG_{01} beam with $w_0=100$ μm. The twin photon source is a PPLN sample of length $L=1$ mm and the wavelength is $\lambda_p^0=406$ nm.

For configurations where the pump, signal, and idler propagate coaxially, one has $\varphi_1=\varphi_2=0$, $\varphi_1=\varphi_2=\pi$ or $\varphi_1=0$, $\varphi_2=\pi$ hence, the spectral properties of the down-converted photons do not depend on the beam width ($\alpha=0$), and thus the spectrum of the generated photons is mainly determined by the length of the nonlinear crystal. Figure 2(a) corresponds to two configurations where the signal and idler photons are copropagating or backward propagating coaxially with the pump beam, as shown in the corresponding inset. In Fig. 2(b) we show that the spectral width for the case where the signal and idler photons counterpropagate is highly reduced, as is the case when the photons are emitted in a waveguide with periodic nonlinearity [8]. Notice that in all these cases the spectrum is independent of the spatial shape of the pump beam.

In contrast, for so-called transverse-emitting configurations, where the down-converted photons are emitted orthogonally to the direction of propagation of the pump beam ($\varphi_2=-\varphi_1=\pi/2$), the spectral properties of the generated two-photon state are determined by the amplitude distribution of the pump beam, since one has $\beta=0$ and $\gamma=0$. Actually, the

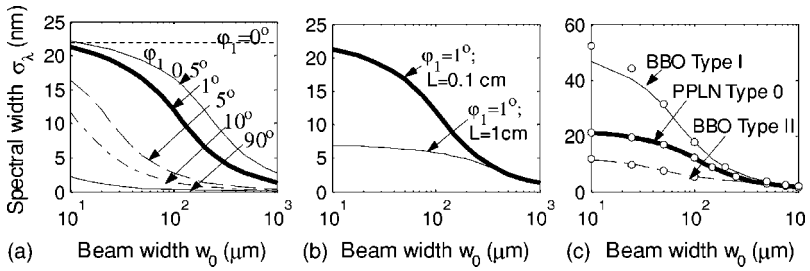

FIG. 4. Spectral width σ_λ of the down-converted photons versus the pump beam width w_0 for degenerate SPDC. (a) PPLN sample for several selected output signal and idler angles, $L=1$ mm. (b) PPLN sample with fixed output angles ($\varphi_1=1°$) and two crystal lengths $L=1$ mm and $L=1$ cm. (c) Fixed output angle ($\varphi_1=1°$) and crystal length ($L=1$ mm) for different types of phase matching. Circles correspond to the approximate expression of the state function given by Eq. (9). In these plots, the wavelength is $\lambda_p^0=406$ nm. In all cases, the pump beam is assumed to be Gaussian.

spectrum of the two-photon state mimics the amplitude distribution of the pump beam. In Fig. 3(a) we show a sketch of a $2f$ configuration to map the spatial properties of the pump beam into the frequency properties of the down-converted photons. One obtains from Eq. (9) that $\Psi(\Omega_s)\simeq\overline{E}_p[0, -\lambda_p^0 f\alpha\Omega_s/(2\pi)]$, where f is the focal length of the system. $\lambda_p^0 f\alpha/(2\pi)$, which depends on the material characteristics and the direction of propagation, is a mapping factor that scales the amplitude distribution of the pump beam when imprinted on the spectral shape of the down-converted photons. In Fig. 3(b) we plot the spectrum obtained for a Gaussian pump beam with width w_0—i.e., $\overline{E}_p(\mathbf{q}_p)\propto\exp(-|\mathbf{q}_p|^2w_0^2/4)$. One finds that in this case the spectral width σ_λ of the state function for a transverse-emitting configuration is given by

$$\sigma_\lambda=\frac{2(\lambda_p^0)^2}{\alpha\pi c w_0}. \tag{11}$$

As shown in Fig. 3(b), a very narrow bandwidth can be achieved. In the case considered here, for beam widths $w_0>25$ μm, subnanometer spectral widths of the state function are obtained. In Fig. 3(c), we plot the spectrum corresponding to a pump beam with the multi-peak spatial distribution: $\overline{E}_p(\mathbf{q}_p)\propto q_y\exp(-|\mathbf{q}_p|^2w_0^2/4)$, which corresponds to a Hermite-Gauss pump beam. The potential of the scheme to tailor the spectral properties of the two-photon state independently of the length of the crystal is clearly apparent.

Finally, Fig. 4 shows the spectral width σ_λ, as a function of the spatial width of a Gaussian pump beam, for several directions of propagation of the signal and idler photons ($\varphi_1=-\varphi_2$) and several crystal lengths. Figures 4(a) and 4(b) correspond to periodically poled lithium niobate (PPLN). The plots show how controlling the beam width impacts the spectral width of the two-photon state. As shown in Fig. 4(b), for large beam widths, the spectral width of the two-photon state is the same for different crystal lengths, and is determined by the angle of propagation. Generally speaking, similar conclusions are obtained for other types of phase matching. In Fig. 4(c) we compare the spectral width calculated for several types of phase matching: *eee* interaction in PPLN (type 0), degenerate type-II phase matching in BBO, and degenerate type-I phase matching in BBO [15]. For all noncollinear configurations, the spectral width decreases with increasing angle of propagation φ_1 and increasing beam width of the pump beam. The main difference between different types of phase matching is the maximum size of the spectral width that can be achieved, as shown in Fig. 4(c). The plot also provides information about the accuracy of the approximate expression given by Eq. (9), when compared with the exact spectrum, as given by Eq. (8). The experimental values reported [16] for nearly collinear type-II phase matching, with a BBO crystal of length $L=2$ mm and photons collected in monomode fibers, agree qualitatively with the values calculated here. For collinear type-II phase matching, the corresponding spectral widths calculated are close to the noncollinear ones.

In conclusion, we have shown that the use of noncollinearly phase-matched SPDC in suitable materials represents a powerful tool for managing the spectral width of two-photon quantum states. In particular, we have shown that in so-called transverse-emitting geometries (i.e., down-converted light emitted perpendicular to the pump-beam direction), the frequency spectrum mimics the spatial amplitude distribution of the pump beam. This allows, for example, the generation of pairs of photons with arbitrary state function shapes and with reduced spectral width. We have also shown that in the commonly used nearly collinear configurations, the width of the pump beam can noticeably change the spectral width of the down-converted photons, a feature to be taken into account when devising practical schemes for enhancing the amount of entanglement in polarization and spatial-entanglement protocols.

This work was supported by the Fulbright Program and the Spanish Ministry of Education and Science; by the Generalitat de Catalunya; by Grant No. BFM2002-2861 from the Government of Spain; by the Center for Subsurface Sensing and Imaging Systems (CenSSIS), a U.S. National Science Foundation Engineering Research Center; and by the David & Lucile Packard Foundation.

[1] *The Physics of Quantum Information*, edited by D. Bouwmeester, A. Ekert, and A. Zeilinger (Springer-Verlag, Berlin, 2000).
[2] N. Gisin, Rev. Mod. Phys. **74**, 145 (2002).
[3] V. Giovannetti, S. Lloyd, and L. Maccone, Nature (London) **412**, 417 (2001); V. Giovannetti, L. Maccone, J. H. Shapiro, and F. N. C. Wong, Phys. Rev. Lett. **88**, 183602 (2002).
[4] W. P. Grice, A. B. U'Ruen, and I. A. Walmsley, Phys. Rev. A **64**, 063815 (2001).
[5] D. Branning, W. P. Grice, R. Erdmann, and I. A. Walmsley, Phys. Rev. Lett. **83**, 955 (1999).
[6] A. F. Abouraddy, M. B. Nasr, B. E. A. Saleh, A. V. Sergienko, and M. C. Teich, Phys. Rev. A **65**, 053817 (2002); M. B. Nasr, B. E. A. Saleh, A. V. Sergienko, and M. C. Teich, Phys. Rev. Lett. **91**, 083601 (2003).
[7] A. De Rossi and V. Berger, Phys. Rev. Lett. **88**, 043901 (2002).
[8] M. C. Booth, M. Atatüre, G. Di Giuseppe, B. E. A. Saleh, A. Sergienko, and M. C. Teich, Phys. Rev. A **66**, 023815 (2002).
[9] Z. D. Walton, M. C. Booth, A. V. Sergienko, B. E. A. Saleh, and M. C. Teich, Phys. Rev. A **67**, 053810 (2003).
[10] A. B. U'Ren, E. Mukamel, K. Banaszek, and I. A. Walmsley, Philos. Trans. R. Soc. London, Ser. A **361**, 1493 (2003).
[11] D. N. Klyshko, Sov. Phys. JETP **28**, 522 (1969).
[12] B. E. A. Saleh, A. F. Abouraddy, A. V. Sergienko, and M. C. Teich, Phys. Rev. A **62**, 043816 (2000). J. P. Torres, C. I. Osorio, and L. Torner, Opt. Lett. **29**, 1939 (2004).
[13] T. E. Keller and M. H. Rubin, Phys. Rev. A **56**, 1534 (1997).
[14] L. Gallmann, G. Steinmeyer, G. Imeshev, J. P. Meyn, M. M. Fejer, and U. Keller, Appl. Phys. B: Lasers Opt. **74**, S237 (2002), and references therein.
[15] D. Eimerl, L. Davis, S. Velsko, E. K. Graham, and A. Zalkin, J. Appl. Phys. **62**, 1968 (1987).
[16] P. Trojek, C. Schmid, M. Bourennane, H. Weinfurter, and C. Kurtsiefer, Opt. Express **12**, 276 (2004). An almost Gaussian distribution with full width half maximum (FWHM) of $\simeq 6$ nm was measured at the degenerate frequency 805.2 nm. The external angles of emission of the downcoverted photons are $\varphi_1 = -\varphi_2 \simeq 3°$.